Solid State Ionics 315 (2018) 65–70

Contents lists available at ScienceDirect

Solid State Ionics

journal homepage: www.elsevier.com/locate/ssi

Hybrid solid electrolytes composed of poly(1,4-butylene adipate) and lithium aluminum germanium phosphate for all-solid-state Li/$LiNi_{0.6}Co_{0.2}Mn_{0.2}O_2$ cells

Myung-Soo Park, Yun-Chae Jung, Dong-Won Kim*

Department of Chemical Engineering, Hanyang University, Seongdong-Gu, Seoul 04763, Republic of Korea

ARTICLE INFO

Keywords:
Poly(1,4-butylene adipate)
Solid electrolyte
All-solid-state battery
Lithium aluminum germanium phosphate
Cycling performance

ABSTRACT

Solid polymer electrolytes based on poly(1,4-butylene adipate) (PBA) and $LiClO_4$ were hybridized with Li^+-conductive lithium aluminum germanium phosphate ($Li_{1.5}Al_{0.5}Ge_{1.5}(PO_4)_3$, LAGP) to obtain highly conductive and flexible solid electrolyte film. Ionic conductivity, mechanical property and electrochemical stability were enhanced by incorporating an appropriate amount of LAGP into the PBA-based solid polymer electrolyte, and the optimum content of LAGP in the hybrid solid electrolytes was approximately 60–80 wt%. The all-solid-state Li/$LiNi_{0.6}Co_{0.2}Mn_{0.2}O_2$ cell employing the optimized hybrid solid electrolyte exhibited an initial discharge capacity of 169.5 mAh g^{-1} with good capacity retention at 55 °C.

1. Introduction

Lithium-ion battery (LIB) has been a leading energy storage technology over the past decades because of its high energy density and long cycle life, and it is being widely used in portable electronics, electric vehicles and energy storage systems [1–5]. However, highly flammable solvents used in the liquid electrolyte still prevent the full utilization of LIBs for existing small power sources and future large-scale applications due to the risk of solvent leakage and fire explosions. In this respect, the all-solid-state lithium batteries employing solid electrolytes have been actively studied in order to enhance the safety of current LIBs [6–13]. Among a variety of solid electrolytes, solid polymer electrolytes possess a lot of potential advantages, including the absence of solvent leakage, good interfacial contacts with electrodes, low cost, easy processing, flexibility and good film formability [6–9]. Solid polymer electrolytes based on poly(ethylene oxide) (PEO) have been intensively studied so far, because PEO can solvate various lithium salts through interaction of its ether oxygens with cations. However, their low ionic conductivities at ambient temperature preclude their practical applications for use in lithium batteries that operate at room temperature. Moreover, the oxidative stability of PEO-based solid polymer electrolytes is still unsatisfactory for applying them to high voltage cathode materials such as $LiCoO_2$, $LiMn_2O_4$ and $LiNi_xCo_yMn_{1-x-y}O_2$ [10]. As an alternative to PEO-based solid polymer electrolytes, polyester-based solid polymer electrolytes have been studied and reported, because ester groups (-COO-) in the polymer backbone can dissolve the lithium salts to produce a sufficient number of free ions and they exhibit higher oxidative stability than ether groups [14–22]. In addition to solid polymer electrolytes, inorganic electrolytes have also been extensively studied as a solid electrolyte for all-solid-state lithium batteries due to their high ionic conductivity, high thermal stability, non-flammability, excellent electrochemical stability and high mechanical strength [11–13]. Among the inorganic electrolytes reported so far, lithium aluminum germanium phosphate ($Li_{1.5}Al_{0.5}Ge_{1.5}(PO_4)_3$, LAGP), one of the NASICON-type solid-state lithium ion conductors, has several advantages such as high ionic conductivity, easy synthesis, superior chemical stability with lithium metal and high electrochemical stability [23–27]. However, the lack of flexibility due to their hard and brittle nature results in inferior interfacial contacts and high interfacial resistance with electrode materials in the cells. Therefore, it is great urgency to develop the flexible solid electrolytes satisfying both high ionic conductivity and improved interfacial contact for realization of all-solid-state lithium batteries [28–30].

In the present work, we prepared flexible hybrid solid electrolytes composed of poly(1,4-butylene adipate) (PBA)-based solid polymer electrolyte and Li^+-conductive LAGP, which exhibited superior electrochemical properties and good interfacial contact towards electrodes in the cell. The hybrid solid electrolyte in the form of flexible thin film was employed for fabricating the all-solid-state Li/$LiNi_{0.6}Co_{0.2}Mn_{0.2}O_2$ cells, and their cycling performance was evaluated. In our work, $LiNi_{0.6}Co_{0.2}Mn_{0.2}O_2$ was chosen as an active material in the composite positive electrode, because it exhibits a high operating voltage and has

* Corresponding author.
E-mail address: dongwonkim@hanyang.ac.kr (D.-W. Kim).

https://doi.org/10.1016/j.ssi.2017.12.007
Received 18 August 2017; Received in revised form 20 November 2017; Accepted 5 December 2017

Table 1
Composition of LAGP, PBA and $LiClO_4$ in different solid electrolytes.

Electrolyte	LAGP (g)	PBA (g)	$LiClO_4$ (g)	[BA]: [Li^+]
PBA/$LiClO_4$	0	2.0	0.177	6: 1
LAGP-60	1.2	0.8	0.071	6: 1
LAGP-70	1.4	0.6	0.053	6: 1
LAGP-80	1.6	0.4	0.035	6: 1
LAGP-90	1.8	0.2	0.018	6: 1

a higher specific capacity and lower cost than $LiCoO_2$. To the best of our knowledge, we report for the first time the cycling characteristics of all-solid-state lithium cells employing a high-voltage $LiNi_{0.6}Co_{0.2}Mn_{0.2}O_2$ cathode material and polyester-based hybrid solid electrolyte.

2. Experimental

2.1. Hybrid solid electrolyte

$Li_{1.5}Al_{0.5}Ge_{1.5}(PO_4)_3$ powders were synthesized by solid solution method, as reported earlier [31]. PBA (average M_w = 12,000), lithium perchlorate ($LiClO_4$) and dimethyl carbonate (DMC) were purchased from Sigma-Aldrich. A hybrid solid electrolyte was prepared using LAGP, PBA and $LiClO_4$, with a composition given in Table 1. PBA and $LiClO_4$ were mixed with a fixed molar ratio of 6:1 for [BA]: [Li^+] in anhydrous DMC at 60 °C for 12 h. LAGP powder with a different weight ratio (60, 70, 80 and 90 wt%) was added to the polymer solution, and the resulting solution was further mixed for 24 h. After complete mixing of the solution, it was cast with a doctor blade onto a flat Teflon plate, and left to evaporate the solvent slowly at room temperature in a glove box under argon atmosphere. The cast film was further dried in a vacuum oven at 60 °C for 12 h to completely remove remaining DMC. After drying process, the free-standing flexible thin film was obtained as a solid-state electrolyte, as depicted in the right side of Fig. 1.

2.2. Li/$LiNi_{0.6}Co_{0.2}Mn_{0.2}O_2$ cell

A composite positive electrode on aluminum current collector consisted of $LiNi_{0.6}Co_{0.2}Mn_{0.2}O_2$, PBA, $LiClO_4$ and Super P carbon in the weight ratio of 60: 27.56: 2.44: 10. Solid polymer electrolyte (PBA/$LiClO_4$) in the composite positive electrode was used as a Li^+-conducting electrolyte as well as a polymer binder. The mass loading of $LiNi_{0.6}Co_{0.2}Mn_{0.2}O_2$ in the composite positive electrode was approximately 6.0 mg cm^{-2}. A lithium foil (200 μm, Honjo Metal Co., Ltd.) pressed onto a copper current collector was used as a negative electrode. The Li/$LiNi_{0.6}Co_{0.2}Mn_{0.2}O_2$ cell was then assembled with hybrid solid electrolyte in CR2032 coin-type cell, as schematically illustrated in the left side of Fig. 1. The cell assembly was conducted in a glove box filled with high-purity argon gas (H_2O < 20 ppm).

2.3. Characterization and measurements

Attenuated total reflectance Fourier transform infrared (ATR-FTIR) spectra were recorded on a Nicolet iS50 spectrometer in the range of 400–4000 cm^{-1}. In order to examine the cross-sectional morphologies of the hybrid solid electrolyte, it was cut using a cross section polisher (JEOL IB-09020CP) at constant power in an inert Ar atmosphere. The cross-sectional image was obtained using field emission scanning electron microscopy (FE-SEM, JEOL JSM-7001F). Energy dispersive X-ray spectroscopy (EDS) was performed to investigate the cross-sectional elemental distribution in the hybrid solid electrolyte. X-ray diffraction (XRD) measurements were performed by X-ray diffractometer (Rigaku M2500) using Cu Kα radiation. The ionic conductivity of the solid electrolytes was determined from AC impedance measurements using a Zahner Electrik IM6 impedance analyzer over the frequency range from 10 Hz to 1 MHz with an amplitude of 10 mV at different temperatures. The solid electrolytes were sandwiched between two disk-like stainless steel blocking electrodes and sealed in Swagelok-type airtight cells. Before the measurements, each sample was stored at the required temperature for at least 1 h. To investigate the oxidative stability of the solid electrolytes, linear sweep voltammetry (LSV) was performed on a platinum working electrode, with lithium metal as reference and counter electrodes, at a scan rate of 1.0 m$V\,s^{-1}$ at 55 °C. Cycling test of the all-solid-state Li/$LiNi_{0.6}Co_{0.2}Mn_{0.2}O_2$ cells was carried out at a constant current rate of 0.2 C within the voltage range between 3.0 and 4.2 *V* using a battery cycler (WBCS 3000, Wonatech) at 55 °C, unless otherwise specified.

3. Results and discussion

To investigate the ion conduction behavior of PBA-based solid polymer electrolytes, their ionic conductivities were measured as a function of salt concentration at room temperature, and the results are shown in Fig. 2(a). The ionic conductivity reached a maximum value at a salt concentration of 2: 1 for [BA]: [Li^+], followed by a decrease with a further increase in $LiClO_4$ concentration. This result is due to two opposing effects on the ionic conductivity, as previously reported [32–34]. Since the carbonyl group in the PBA backbone is a strong electron donor and it can effectively dissociate the lithium salt, there is a buildup of free ions as the salt concentration increases. However, this is eventually offset by the increase in ion-polymer interactions and the consequential reduction in ionic mobility at high salt concentration. Ion-polymer interactions and the dissociation of the salt in the PBA-based solid polymer electrolytes were examined by ATR-FTIR spectroscopy, and the resulting spectra are shown in Fig. 2(b) and (c). In Fig. 2(b), the main peak observed at 1730 cm^{-1} in pure PBA corresponds to the free carbonyl stretching, and the peak appearing at 1700 cm^{-1} in the solid polymer electrolytes can be assigned to Li^+-coordinating carbonyl stretching [21]. The intensity of the peak at

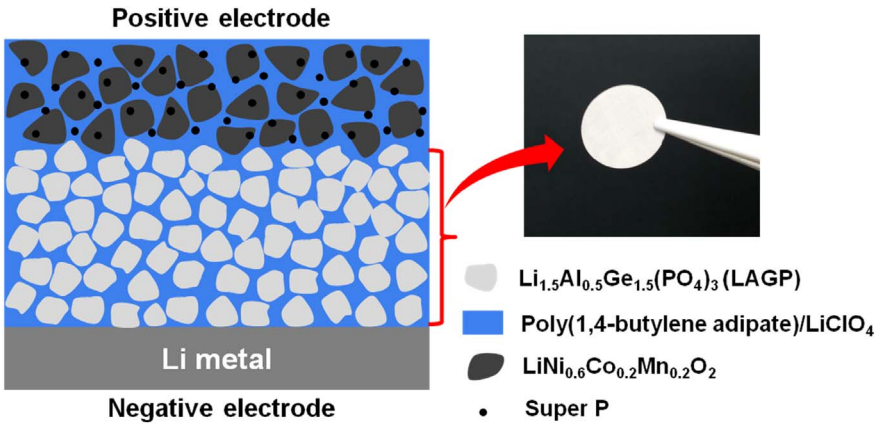

Fig. 1. Schematic presentation of the all-solid-state Li/$LiNi_{0.6}Co_{0.2}Mn_{0.2}O_2$ cell employing hybrid solid electrolyte and photo image of a representative hybrid solid electrolyte (LAGP-70).

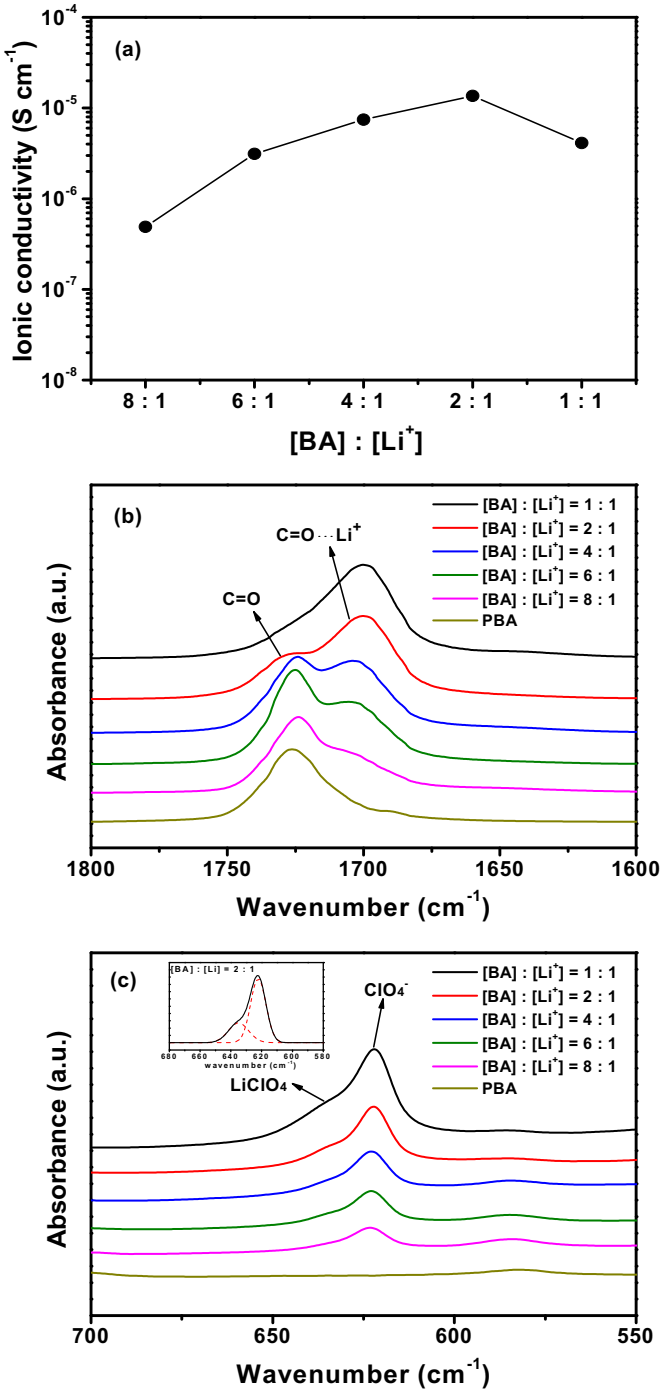

Fig. 2. (a) Ionic conductivities of PBA-based solid polymer electrolytes as a function of salt concentration at 25 °C. ATR-FTIR spectra of the PBA-based solid polymer electrolytes with different salt concentrations in the different wavenumber ranges of (b) 1600–1800 cm^{-1} and (c) 550–700 cm^{-1}.

1730 cm^{-1} gradually decreases and the peak intensity at 1700 cm^{-1} increases with increasing $LiClO_4$ concentration, indicating effective complexation of $LiClO_4$ by carbonyl groups in PBA. In Fig. 2(c), the peaks at 635 and 623 cm^{-1} correspond to the contact ion-pairs of $LiClO_4$ and the dissociated ClO_4^- anion, respectively [21]. To estimate the dissociation degree of the salt, the peak in the region of 570 to 680 cm^{-1} was decomposed with two Gaussian peaks, as shown in the inset of Fig. 2(c). As a result, the relative ratio of free ions to contact ion-pairs decreased from 72.8 to 52.4%, as the salt concentration ([BA]: $[Li^+]$) increased from 8:1 to 1:1 in the solid polymer electrolyte,

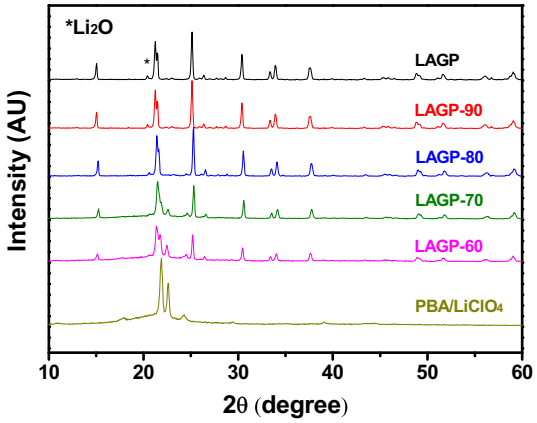

Fig. 3. XRD patterns of LAGP powder, various hybrid solid electrolytes (from LAGP-60 to LAGP-90), and PBA-based solid polymer electrolyte.

indicating that the relative fraction of dissociated free ions decreases with salt concentration. Despite the highest ionic conductivity for the PBA-based solid polymer electrolyte at a salt concentration of [BA]: $[Li^+]$ = 2: 1, it was not a free-standing but gel-like film, and thus its dimensional stability was not good for preparing the hybrid solid electrolyte film. Thus, we choose the free-standing solid polymer electrolyte with a salt concentration of [BA]: $[Li^+]$ = 6: 1 for hybridization with LAGP powder in further experiments.

Fig. 3 presents the XRD patterns of LAGP, various hybrid solid electrolytes (from LAGP-60 to LAGP-90) and the PBA-based solid polymer electrolyte ($PBA/LiClO_4$). The crystalline peaks of LAGP are consistent with those of NASICON-type $LiGe_2(PO_4)_3$ (JCPDS 80–1924) [23,31]. The XRD pattern of the $PBA/LiClO_4$ shows two sharp and one broad crystalline peaks at 2θ = 21.9, 22.6 and 24.3°, respectively, which are corresponding to the thermodynamically stable α crystalline phase of PBA [35,36]. When the $PBA/LiClO_4$ was hybridized with LAGP, the crystalline peaks in PBA was reduced, which can be ascribed to the disorder of the polymer chains due to the destruction effect of the LAGP powder. It is well known that the addition of ceramic fillers, such as Al_2O_3, SiO_2 and TiO_2, effectively decrease the crystalline phase in the solid polymer electrolytes by introducing the topological disorder [37–39].

A cross-sectional FE-SEM image of LAGP-70 is shown in Fig. 4(a). The image shows the homogeneous embedment of LAGP particles, which are surrounded by the polymer electrolyte ($PBA/LiClO_4$) phase. Fig. 4(b) presents the EDS mapping images of different elements (Ge, P, C and Cl) on the cross-section of LAGP-70. The Ge and P elements arising from LAGP powder are observed to be uniformly distributed in the image. Both C and Cl elements coming from the $PBA/LiClO_4$ phase are also homogeneously dispersed across the hybrid solid electrolyte. Such a uniform distribution of LAGP and $PBA/LiClO_4$ enables facile migration of Li^+ ions in the hybrid solid electrolyte. It is notable that interfacial contact between the hybrid solid electrolyte and Li metal is very firm without external pressure, which cannot be achieved on the interface between LAGP pellet and lithium metal.

The temperature dependence of the ionic conductivity for different hybrid solid electrolytes (LAGP-60, LAGP-70, LAGP-80, LAGP-90) and PBA-based solid polymer electrolyte ($PBA\text{-}LiClO_4$) was investigated and presented in Fig. 5(a). It is found that the ionic conductivity depends on the content of LAPG in the hybrid solid electrolyte. As shown in the figure, increasing the LAGP content from 60 to 70 wt% increased the ionic conductivity over all temperature ranges investigated, however a further increase in LAGP content over 70 wt% decreased the ionic conductivity. As mentioned earlier, the hybridization of PBA and LAGP reduced the crystallinity of the solid polymer electrolyte because LAGP particles suppressed the ordering of polymer chains, which resulted in increase of ionic conductivity [39]. Fast migration of lithium ions in

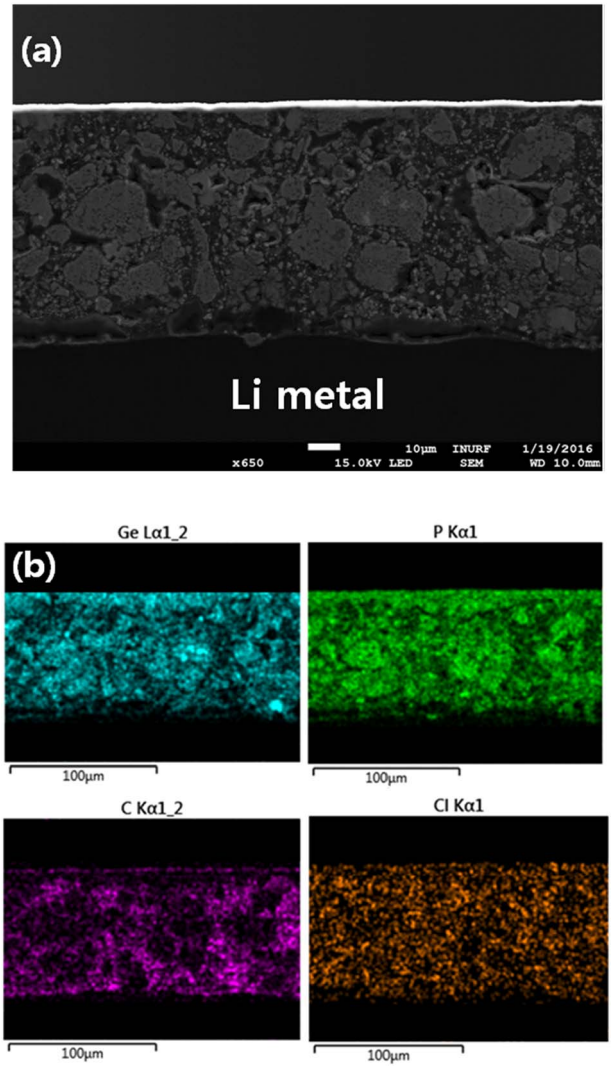

Fig. 4. (a) Cross-sectional SEM image of LAGP-70, and (b) EDS mapping images of Ge, P, C, and Cl on the cross section of LAGP-70.

LAGP particles, a kind of superionic conductor with high lithium ion conductivity, also enhanced the ionic conduction. The ionic conductivity of LAGP pellet with a thickness of 1000 μm was 1.9×10^{-4} S cm^{-1} at room temperature. However, the excessive addition of LAGP over 70 wt% resulted in a decrease in the ionic conductivity. It should be noted that LAGP in the powder form without high-temperature sintering exhibited high ionic resistance due to large grain boundary resistance as well as poor interfacial contacts between LAGP particles. When the LAPG content was > 70 wt%, the interfacial contact between the LAGP particles and solid polymer electrolyte (PBA/$LiClO_4$) for facile transport of Li^+ ions was poor, which resulted in an increase of ionic resistance. The activation energy for ionic conduction in the solid electrolytes was calculated using $\sigma = A \exp.(-E_a/kT)$, where A is the pre-exponential constant, E_a is the activation energy, k is the Boltzmann constant, and T is the absolute temperature. The activation energies of the hybrid solid electrolytes in the lower temperature region (25–45 °C) are calculated to be in the range of 53.4–68.4 kJ mol^{-1}, which are much lower than that of the PBA-based solid polymer electrolyte (88.0 kJ mol^{-1}). This result can be ascribed to the high crystallization tendency of PBA at lower temperatures. In a higher temperature region (55–75 °C), the activation energy in the solid polymer electrolyte was significantly reduced, indicating that the melting of crystalline PBA promoted faster ion transport through the amorphous phase of the solid polymer electrolyte. Though the PBA-based solid

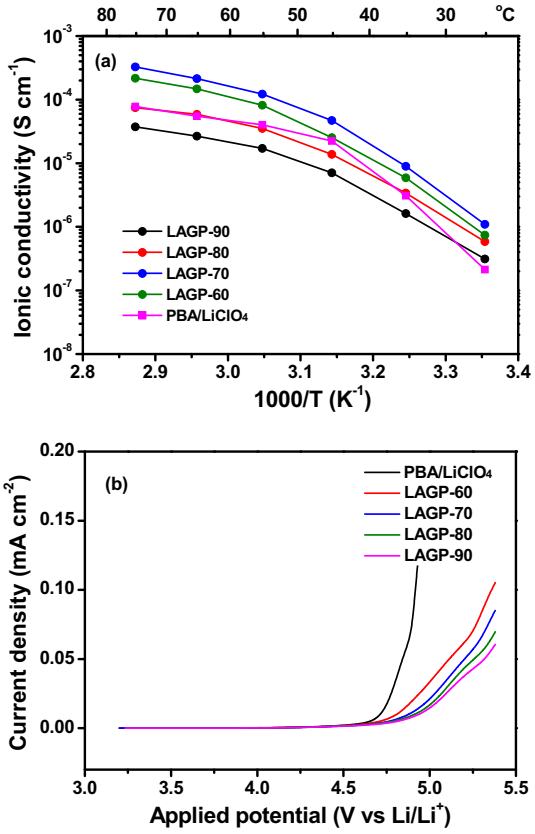

Fig. 5. (a) Temperature dependence of the ionic conductivity for various solid electrolytes, and (b) linear sweep voltammograms of different solid electrolytes (55 °C, scan rate: 1 mV s^{-1}).

polymer electrolyte without LAGP exhibited enhanced ionic conductivities with increasing temperature, its mechanical properties were not good due to the melting of the crystalline PBA phase in the higher temperature region. The anodic stability of the various solid electrolytes was examined by using linear sweep voltammetry at 55 °C, and the results are shown in Fig. 5(b). It should be noted that the measurements were performed at 55 °C, because the ionic conductivities of the solid electrolytes were so low at ambient temperature, that we could not measure and compare the oxidative current at that temperature. As shown in the figure, the oxidative current showed an abrupt rise around 4.7 V vs. Li/Li^+ in the PBA-based solid polymer electrolyte, which can be ascribed to the electrochemical oxidative decomposition of PBA. On the other hand, the hybrid solid electrolytes exhibited superior electrochemical stability compared to the PBA-based solid polymer electrolyte, indicating that introducing LAPG into the PBA-based polymer electrolyte enhanced the oxidative stability. This result can be ascribed to the high electrochemical stability of LAGP [25]. On the basis of these results, it is anticipated that the hybrid solid electrolytes have high oxidative stability for electrochemical operation of the Li/$LiNi_{0.6}Co_{0.2}Mn_{0.2}O_2$ cell that is cycled in the high voltage range of 3.0–4.2 V.

An all-solid-state Li/$LiNi_{0.6}Co_{0.2}Mn_{0.2}O_2$ cell was fabricated using the flexible hybrid solid electrolyte. Among the hybrid solid electrolytes investigated above, LAGP-90 was not applied to the cell due to the high ionic resistance of the electrolyte and the poor interfacial contacts between the electrolyte and electrodes in the cell. The solid-state Li/$LiNi_{0.6}Co_{0.2}Mn_{0.2}O_2$ cells were charged and discharged at 0.2C rate and 55 °C. Fig. 6(a) shows the voltage profiles of the Li/$LiNi_{0.6}Co_{0.2}Mn_{0.2}O_2$ cell employing LAGP-70 with the repeated cycling. The cell exhibited an initial discharge capacity of 169.5 mAh g^{-1} based on the active $LiNi_{0.6}Co_{0.2}Mn_{0.2}O_2$ material in the positive electrode, with a

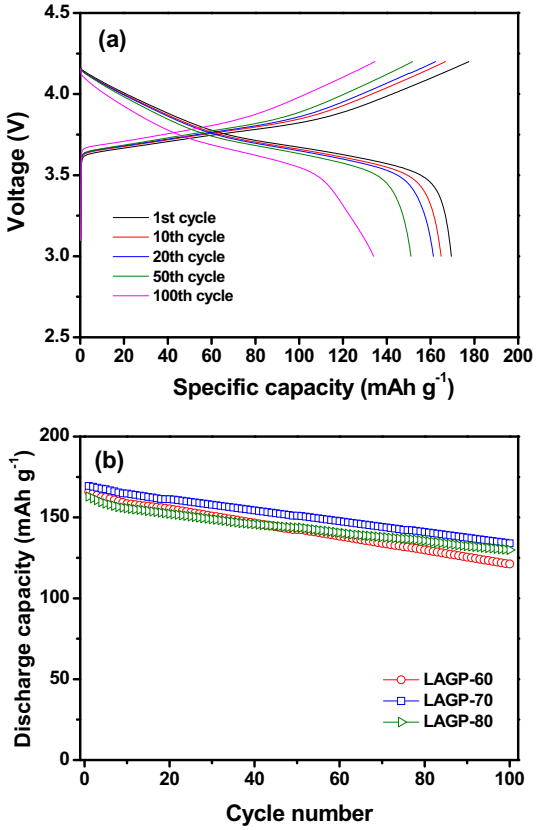

Fig. 6. (a) Galvanostatic charge and discharge curves of the all-solid-state Li/$LiNi_{0.6}Co_{0.2}Mn_{0.2}O_2$ cell assembled with LAGP-70, and (b) variation of discharge capacities of the all-solid-state Li/$LiNi_{0.6}Co_{0.2}Mn_{0.2}O_2$ cells with cycle number at 0.2C rate (cut-off voltage: 3.0–4.2 V, temperature: 55 °C).

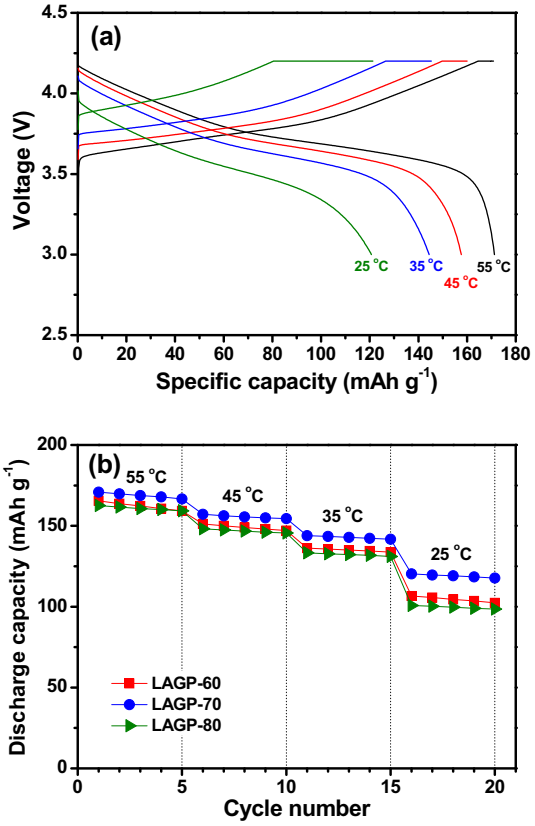

Fig. 7. (a) First charge and discharge curves of the all-solid-state Li/$LiNi_{0.6}Co_{0.2}Mn_{0.2}O_2$ cell assembled with LAGP-70 at different temperatures, and (b) discharge capacities of the all-solid-state Li/$LiNi_{0.6}Co_{0.2}Mn_{0.2}O_2$ cells cycled at different temperature.

coulombic efficiency of 95.5%. This initial discharge capacity is very close to that (~170.8 mAh g^{-1}) obtained in the Li/$LiNi_{0.6}Co_{0.2}Mn_{0.2}O_2$ cell employing conventional liquid electrolyte (1.0 M $LiPF_6$ in ethylene carbonate/dimethyl carbonate, 1:1 by volume) at 25 °C. The coulombic efficiency steadily increased with cycling to reach a constant value of over 99.5% throughout cycling after the initial few cycles. Fig. 6(b) shows the discharge capacities of the Li/$LiNi_{0.6}Co_{0.2}Mn_{0.2}O_2$ cells employing different hybrid solid electrolytes. Although the cell assembled with LAGP-80 delivered the lowest initial discharge capacity (162.9 mAh g^{-1}), it exhibited the best cycling stability. This result is due to the fact that the use of the electrochemically stable solid electrolyte (LAGP-80) containing a high amount of LAGP suppresses detrimental side reactions at the electrolyte-electrode interfaces, which gives in better cycling stability.

The cycling test of the all-solid-state Li/$LiNi_{0.6}Co_{0.2}Mn_{0.2}O_2$ cells was performed at various temperatures, with decreasing temperature from 55 to 25 °C. In order to examine the cycling behavior of the cells at different temperatures, the cells were charged at a constant current rate of 0.2C up to a cut-off voltage of 4.2 *V* at measured temperature. This was followed by constant voltage charging until the final current reached 10% of the charging current. Cells were then discharged to a cut-off voltage of 3.0 V at the same current rate (0.2 C). These charge and discharge cycles were repeated five times at the same temperature. After cycling the test at a given temperature, the temperature was decreased at an interval of 10 °C, and the same test condition was applied to the cell. Fig. 7(a) shows the voltage profiles of the Li/$LiNi_{0.6}Co_{0.2}Mn_{0.2}O_2$ cell with LAGP-70, which were obtained for the first cycle at different temperatures. As shown in the figure, the overpotential increased with decreasing temperature, which is mainly due to the increase of ionic resistance in both the hybrid solid electrolyte and composite positive electrode. In addition, the capacity charged during constant-voltage charging increased, indicating that the internal cell resistances increased with decreasing temperature. As a result, the discharge capacity of the cell decreased from 170.8 mAh g^{-1} at 55 °C to 120.3 mAh g^{-1} at 25 °C. Fig. 7(b) shows the discharge capacities of the cells, which were measured every five cycles at different temperatures. As explained above in the cell with LAGP-70, the discharge capacities decreased with decreasing temperature, which was caused by high overpotential at low temperature. It is notable that the cell could deliver relatively high capacity even at room temperature (100.8–120.3 mAh g^{-1}). Although the ionic conductivity of LAGP-70 was low at ambient temperature, the interfacial contacts between solid electrolyte and electrodes were very firm, and thus the interfacial resistance in the cell was not so high. Moreover, a lot of capacity could be restored in the cell during constant voltage charging at 25 °C, as shown in Fig. 7(a). Accordingly, the all-solid-state Li/$LiNi_{0.6}Co_{0.2}Mn_{0.2}O_2$ cell could be operated with reduced capacity when cycling at ambient temperature.

4. Conclusions

Solid polymer electrolytes based on PBA and $LiClO_4$ were prepared, and their electrochemical characteristics were evaluated. Ionic conductivity, mechanical property and electrochemical stability were enhanced by hybridizing the PBA-based solid polymer electrolyte with Li^+ ion-conductive LAGP. All-solid-state Li/$LiNi_{0.6}Co_{0.2}Mn_{0.2}O_2$ cell employing the optimized hybrid solid electrolyte delivered a high discharge capacity of 169.5 mAh g^{-1} and showed good capacity retention at 55 °C. The cell also exhibited relatively high discharge capacity at room temperature, demonstrating the feasibility of using this hybrid solid electrolyte in all-solid-state lithium batteries.

Acknowledgements

This work was supported by the Basic Science Research Program of the National Research Foundation of Korea (NRF), funded by the Ministry of Science, ICT and Future Planning (2014R1A2A2A01002154) and the R&D Convergence Program of the NST (National Research Council of Science & Technology) of the Republic of Korea.

References

[1] J.-M. Tarascon, M. Armand, Issues and challenges facing rechargeable lithium batteries, Nature 414 (2001) 359–367.
[2] M. Armand, J.M. Tarascon, Building better batteries, Nature 451 (2008) 652–657.
[3] B. Dunn, H. Kamath, J.-M. Tarascon, Electrical energy storage for the grid: a battery of choices, Science 334 (2011) 928–935.
[4] V. Etacheri, R. Marom, R. Elazari, G. Salitra, D. Aurbach, Challenges in the development of advanced Li-ion batteries: a review, Energy Environ. Sci. 4 (2011) 3243–3262.
[5] D. Larcher, J.-M. Tarascon, Towards greener and more sustainable batteries for electrical energy storage, Nat. Chem. 7 (2015) 19–29.
[6] M.B. Armand, The history of polymer electrolytes, Solid State Ionics 69 (1994) 309–319.
[7] K. Murata, S. Izuchi, Y. Yoshihisa, An overview of the research and development of solid polymer electrolyte batteries, Electrochim. Acta 45 (2000) 1501–1508.
[8] J.W. Fergus, Ceramic and polymeric solid electrolytes for lithium-ion batteries, J. Power Sources 195 (2010) 4554–4569.
[9] E. Quartarone, P. Mustarelli, Electrolytes for solid-state lithium rechargeable batteries: recent advances and perspectives, Chem. Soc. Rev. 40 (2011) 2525–2540.
[10] Y.-C. Jung, S.-M. Lee, J.-H. Choi, S.-S. Jang, D.-W. Kim, All solid-state lithium batteries assembled with hybrid solid electrolytes, J. Electrochem. Soc. 162 (2015) A704–A710.
[11] P. Knauth, Inorganic solid Li ion conductors: an overview, Solid State Ionics 180 (2009) 911–916.
[12] N. Kamaya, K. Homma, Y. Yamakawa, M. Hirayama, R. Kanno, M. Yonemura, T. Kamiyama, Y. Kato, S. Hama, K. Kawamoto, A. Mitsui, A lithium superionic conductor, Nat. Mater. 10 (2011) 682–686.
[13] V. Thangadurai, S. Narayanan, D. Pinzaru, Chem. Soc. Rev. 43 (2014) 4714–4727.
[14] M. Watanabe, M. Rikukawa, K. Sanui, N. Ogata, H. Kato, T. Kobayashi, Z. Ohtaki, Ionic conductivity of polymer complexes formed by poly(ethylene succinate) and lithium perchlorate, Macromolecules 17 (1984) 2902–2908.
[15] R.D. Armstrong, M.D. Clarke, Lithium ion conducting polymeric electrolytes based on poly(ethylene adipate), Electrochim. Acta 29 (1984) 1443–1446.
[16] R. Dupon, B.L. Papke, M.A. Ratner, D.F. Shriver, Ion-transport in the polymer electrolytes formed between poly(ethylene succinate) and lithium tetrafluoroborate, J. Electrochem. Soc. 131 (1984) 586–589.
[17] M. Watanabe, M. Rikukawa, K. Sanui, N. Ogata, Effects of polymer structure and incorporated salt species on ionic-conductivity of polymer complexes formed by aliphatic polyester and alkali-metal thiocyanate, Macromolecules 19 (1986) 188–192.
[18] D.-W. Kim, J.-S. Song, J.-K. Park, Synthesis, characterization and electrical properties of the novel polymer electrolytes based on polyesters containing ethylene oxide moiety, Electrochim. Acta 40 (1995) 1697–1700.
[19] Y.C. Lee, M.A. Ratner, D.F. Shriver, Ionic conductivity in the poly(ethylene malonate)/lithium triflate system, Solid State Ionics 138 (2001) 273–276.
[20] T. Uno, S. Kawaguchi, M. Kubo, T. Itoh, Ionic conductivity and thermal property of solid hybrid polymer electrolyte composed of oligo (ethylene oxide) unit and butyrolactone unit, J. Power Sources 178 (2008) 716–722.
[21] C.K. Lin, I.D. Wu, Investigating the effect of interaction behavior on the ionic conductivity of polyester/$LiClO_4$ blend systems, Polymer 52 (2011) 4106–4113.
[22] J. Mindemark, B. Sun, E. Torma, D. Brandell, High-performance solid polymer electrolytes for lithium batteries operational at ambient temperature, J. Power Sources 298 (2015) 166–170.
[23] X. Xu, Z. Wen, X. Wu, X. Yang, Z. Gu, Lithium ion-conducting glass-ceramics of $Li_{1.5}Al_{0.5}Ge_{1.5}(PO_4)_3$-$xLi_2O$(x = 0.0 − 0.20) with good electrical and electrochemical properties, J. Am. Ceram. Soc. 90 (2007) 2802–2806.
[24] J.S. Thokchom, B. Kumar, Composite effect in superionically conducting lithium aluminium germanium phosphate based glass-ceramic, J. Power Sources 185 (2008) 480–485.
[25] J.K. Feng, L. Lu, M.O. Lai, Lithium storage capability of lithium ion conductor $Li_{1.5}Al_{0.5}Ge_{1.5}(PO_4)_3$, J. Alloys Compd. 501 (2010) 255–258.
[26] H. Chung, B. Kang, Increase in grain boundary ionic conductivity of $Li_{1.5}Al_{0.5}Ge_{1.5}(PO_4)_3$ by adding excess lithium, Solid State Ionics 263 (2014) 125–130.
[27] Z.Q. Liu, S. Venkatachalam, L. van Wullen, Structure, phase separation and Li dynamics in sol-gel-derived $Li_{1+x}Al_xGe_{2-x}(PO_4)_3$, Solid State Ionics 276 (2015) 47–55.
[28] J.-H. Choi, C.-H. Lee, J.-H. Yu, C.-H. Doh, S.-M. Lee, Enhancement of ionic conductivity of composite membranes for all-solid-state lithium rechargeable batteries incorporating tetragonal $Li_7La_3Zr_2O_{12}$ into a polyethylene oxide matrix, J. Power Sources 274 (2015) 458–463.
[29] Y. Zhao, C. Wu, G. Peng, X. Chen, X. Yao, Y. Bai, F. Wu, S. Chen, X. Xu, A new solid polymer electrolyte incorporating $Li_{10}GeP_2S_{12}$ into a polyethylene oxide matrix for all-solid-state lithium batteries, J. Power Sources 301 (2016) 47–53.
[30] Y.-C. Jung, M.-S. Park, C.-H. Doh, D.-W. Kim, Organic-inorganic hybrid solid electrolytes for solid-state lithium cells operating at room temperature, Electrochim. Acta 218 (2016) 271–277.
[31] H.S. Jadhav, M.S. Cho, R.S. Kalubarme, J.S. Lee, K.N. Jung, K.H. Shin, C.J. Park, Influence of B_2O_3 addition on the ionic conductivity of $Li_{1.5}Al_{0.15}(PO_4)_3$ glass ceramics, J. Power Sources 241 (2013) 502–508.
[32] M. Watanabe, J. Ikeda, I. Shinohara, Effect of molecular weight of polymeric solvent on ion conductive behavior in poly(propylene oxide) solution of $LiClO_4$, Polym. J. 15 (1983) 65–69.
[33] R. Xue, C.A. Angell, High ionic conductivity in PEO. PPO block polymer + salt solutions, Solid State Ionics 25 (1987) 223–230.
[34] D.-W. Kim, J.-K. Park, H.-W. Rhee, Conductivity and thermal studies of solid polymer electrolytes prepared by blending poly(ethylene oxide), poly(oligo[oxyethylene] oxysebacoyl) and lithium perchlorate, Solid State Ionics 83 (1996) 49–56.
[35] X. Sun, F. Pi, J. Zhang, I. Takahashi, F. Wang, S. Yan, Y. Ozaki, Study on the phase transition behavior of poly(butylene adipate) in its blends with poly(vinyl phenol), J. Phys. Chem. B 115 (2011) 1950–1957.
[36] E.M. Woo, M.C. Wu, Thermal and X-ray analysis of polymorphic crystals, melting and crystalline transformation in poly(butylene adipate), J. Polym. Sci. B Polym. Phys. 43 (2005) 1662–1672.
[37] J.E. Weston, B.C.J. Steele, Effects of inert fillers on the mechanical and electrochemical properties of lithium salt-poly(ethylene oxide) polymer electrolytes, Solid State Ionics 7 (1982) 75–79.
[38] J. Fan, P.S. Fedkiw, Composite electrolytes prepared from fumed silica, polyethylene oxide oligomers, and lithium salts, J. Electrochem. Soc. 144 (1997) 399–408.
[39] F. Croce, G.B. Appetecchi, L. Persi, B. Scrosati, Nanocomposite polymer electrolytes for lithium batteries, Nature 394 (1998) 456–468.